Single wall and multiwall carbon nanotubes induce different toxicological responses in rat alveolar macrophages

Sara Nahle, Ramia Safar, Stéphanie Grandemange, Bernard Foliguet, Mélanie Lovera-Leroux, Zahra Doumandji, Alain Le Faou, Olivier Joubert, Bertrand Rihn, Luc Ferrari

Received: 17 October 2018 | Revised: 19 November 2018 | Accepted: 19 November 2018

DOI: 10.1002/jat.3765

RESEARCH ARTICLE

WILEY Journal of Applied Toxicology

Single wall and multiwall carbon nanotubes induce different toxicological responses in rat alveolar macrophages

Sara Nahle | Ramia Safar | Stéphanie Grandemange | Bernard Foliguet | Mélanie Lovera-Leroux | Zahra Doumandji | Alain Le Faou | Olivier Joubert | Bertrand Rihn | Luc Ferrari

Toxicology and Molecular Biology, Institute Jean Lamour UMR 7198 du CNRS, Université de Lorraine, F-54000 Nancy, France

Correspondence
Sara Nahle, Toxicology and Molecular Biology, Institute Jean Lamour UMR 7198 du CNRS, Université de Lorraine, F-54000 Nancy, France.
Email: sara.nahle@univ-lorraine.fr

Abstract

Human exposure to airborne carbon nanotubes (CNT) is increasing because of their applications in different sectors; therefore, they constitute a biological hazard. Consequently, developing studies on CNT toxicity become a necessity. CNTs can have different properties in term of length, size and charge. Here, we compared the cellular effect of multiwall (MWCNTs) and single wall CNTs (SWCNTs). MWCNTs consist of multiple layers of graphene, while SWCNTs are monolayers. The effects of MWCNTs and SWCNTs were evaluated by the water-soluble tetrazolium salt cell proliferation assay on NR8383 cells, rat alveolar macrophage cell line (NR8383). After 24 hours of exposure, MWCNTs showed higher toxicity (50% inhibitory concentration [IC_{50}] = 3.2 cm^2/cm^2) than SWCNTs (IC_{50} = 44 cm^2/cm^2). Only SWCNTs have induced NR8383 cells apoptosis as assayed by flow cytometry using the annexin V/IP staining test. The expression of genes involved in oxidative burst (*Ncf1*), inflammation (*Nfκb*, *Tnf-α*, *Il-6* and *Il-1β*), mitochondrial damage (*Opa*) and apoptotic balance (*Pdcd4*, *Bcl-2* and *Casp-8*) was determined. We found that MWCNT exposure predominantly induce inflammation, while SWCNTs induce apoptosis and impaired mitochondrial function. Our results clearly suggest that MWCNTs are ideal candidates for acute inflammation induction. In vivo studies are required to confirm this hypothesis. However, we conclude that toxicity of CNTs is dependent on their physical and chemical characteristics.

KEYWORDS

apoptosis, in vitro, inflammation, multiwall carbon nanotubes, MWCNT, oxidative stress, rat macrophages cell line NR8383, single wall carbon nanotubes, SWCNT

1 | INTRODUCTION

Handling the matter in the range of 1-100 nm allows creating tools and materials with varied physicochemical properties and distinctive features such as firmness, flexibility, opacity, reflexivity, magnetism or antimicrobial activity.

For example, carbon nanotubes (CNTs) offer a huge potential in nano-electronics as semiconductors (Lefebvre et al., 2017). Their high thermal conductivity (Monea et al., 2017), resistance and intrinsic mechanical properties (Dresselhaus, Dresselhaus, Charlier, & Hernández, 2004) such as high tensile strength and flexibility, make them ideal for numerous applications in the biomedical domain, for

instance drug delivery (Assali, Zaid, Abdallah, Almasri, & Khayyat, 2017; Khan et al., 2017; Samadishadlou et al., 2017). CNTs have been widely explored in structural polymer nanocomposites, conductive adhesives, fire retardant plastics, Li-ion battery electrodes and metal matrix composites (Madian et al., 2017; Messina et al., 2016). This brings millions of nanomaterials to the consumer market (Pitkethly, 2004). Consequently, human concerns on the toxicological risks associated with nanoparticle exposure increase.

Indeed, CNTs induce adverse effects, particularly on the respiratory tract, which constitutes the main route for penetration of these nanomaterials. They cause inflammatory, immunologic and fibrogenic effects in rodent lungs (Duke et al., 2017; Qin et al., 2017). Furthermore, key events shown on a cellular level, with NR8383 cells reveal that CNTs play a vital role in cell growth inhibition, production of reactive oxygen species (Fujita et al., 2015) and decrease of the mitochondrial membrane potential (Pulskamp, Diabaté, & Krug, 2007).

However, like other nanomaterials, the physical characteristics of CNTs are very important determinants of their toxicity.

For example, shorter single wall CNTs (SWCNTs) induce greater pulmonary toxicity than longer SWCNTs after intratracheal instillation in rats (Ema et al., 2017). Another study indicates that the longest CNTs were more potent than shorter ones for the production of pro-inflammatory cytokines in the mouse macrophage cell line J774A.1 (Boyles et al., 2015). Therefore, these findings point out that the pulmonary toxicity caused by CNTs is length dependent. Fujita et al. (2015) studied the effect of the CNT size on pulmonary toxicity and showed that longer SWCNTs in thick bundles induce cellular responses in alveolar macrophages and acute lung inflammation, shortly after inhalation, compared to the shortest ones in thin bundles. Moreover, the toxicity of CNTs is also impacted by chemical determinants as metal impurities (Ge et al., 2012) or CNT functionalization (Allegri et al., 2016).

In this context, it was quite interesting to compare the toxicity imposed by CNTs of varied morphology: multiwall short and thick CNTs (MWCNT/NM403 (Poulsen et al., 2016; Vales, Rubio, & Marcos, 2016) and single wall long and thin (SWCNT/NRCWE-055). To the best of our knowledge, this is the first report describing the toxicity of this kind of nanotubes, on NR8383 cells. We chose certain genes that are involved in inflammation, oxidative stress, mitochondrial damage and cell death, to determine precisely the key events of CNT toxicity. In conclusion, we suggested that the type of cell death plays a vital role in the induction of acute inflammation.

2 | MATERIALS AND METHODS

2.1 | Cell culture

NR8383 cells, a rat alveolar macrophage cell line, were obtained from the American Type Culture Collection (ATCC, Manassas, VA, USA). Cells were grown in Dulbecco's modified Eagle medium high glucose (DMEM; Sigma-Aldrich, St. Louis, MO, USA), supplemented with 15% fetal bovine serum (FBS; Sigma-Aldrich), 100 U/mL penicillin and 100 g/mL streptomycin, 4 mM L-glutamine and 0.25 μg/mL of amphotericin B. Cells were grown at 37°C in a 5% CO_2 atmosphere and split every 3 days.

2.2 | Materials dispersion and characterization

MWCNT/NM403 were provided by the Joint Research Center, Belgium and SWCNT/NRCWE-055 by the National Research Centre for the Working Environment (NRCWE), Denmark. CNTs were suspended at 2 mg/mL concentration in DMEM high glucose medium with 2% FBS and sonicated in 5 mL volume, on ice, for 15 minutes, with a Vibra Cell™ Sonicator (20 W; VWR, England, UK) using an 11 mm probe, operated at 10% amplitude.

Size, polydispersity index and zeta potential of CNTs were measured by dynamic light scattering (DLS) with a Malvern Nano Zetasizer (Malvern Inc., Malvern, Worcs, UK), in a cell culture medium (2% FBS). The CNT concentration retained for DLS measurement was 200 μg/mL.

For transmission electron microscopy, a drop of CNT suspension was deposited on to a carbon-coated copper grid. After drying, the sample was negatively stained by uranyl acetate (3%) in deionized water. Preparations were observed under a CM12 microscope (Philips, Amsterdam, The Netherlands) operated at 80 kV. CNT diameters were determined on 114 round objects.

2.3 | Viability tests

2.3.1 | Cell treatment

For the viability tests, NR8383 cells were seeded on to a 96-well plate (5×10^5 cells/well). After 24 hours, the medium was replaced with 100 μL of CNT solutions at different concentrations 2.5, 5, 10, 20, 40 and 80 cm^2/cm^2 (nanoparticle surface/cell surface) for MWCNT/NM403 and 9, 19, 38, 75, 150 and 300 cm^2/cm^2 for SWCNT/NRCWE-055 in DMEM without FBS and without phenol red. These concentrations correspond to mass concentrations of 6, 12.5, 25, 50, 100 and 200 μg/mL respectively. Cells were incubated for 4 and 24 hours, respectively.

2.3.2 | Water-soluble tetrazolium salt assay

The test was performed according to the manufacturer's recommendations using water-soluble tetrazolium salt assay cell proliferation reagent (Roche, Boulogne, France). Absorbance was measured at 450 nm using an iMarK™ microplate reader (Bio-Rad Laboratories, Osaka, Japan). Unexposed cells served as the reference value defining 100% cellular viability.

2.3.3 | Alamar Blue assay

After exposure, 10 μL of Alamar Blue® Reagent (Roche) was added directly to each well. The plates were incubated at 37°C for 3 hours. Fluorescence was measured at excitation/emission wavelengths of 570/600 nm using a FP-8300 Irm spectrofluorometer (Jasco, Lisses, France).

2.3.4 | Lactate dehydrogenase assay

The test was conducted following the manufacturer's instructions using the lactate dehydrogenase (LDH) cytotoxicity detection kit. LDH activity in the supernatant was quantified using an iMarK™ Microplate Reader (Bio-Rad Laboratories) at 490 nm wavelength and 630 nm as the reference wavelength.

2.3.5 | Flow cytometry analysis

NR8383 cells were plated on to six-well culture plates (25×10^4 cells/well), and then exposed to CNTs (2.5, 5, 10, 20 and 40 cm^2/cm^2 for MWCNT/NM403 and 4.5, 9, 19, 38, 75 and 150 cm^2/cm^2 for SWCNT/NRCWE-055) for 4 and 24 hours. Then, cells were harvested and washed twice in phosphate-buffered saline. They were suspended and stained using annexin V and fluorescein isothiocyanate (FITC) apoptosis detection kit (BD Biosciences, Heidelberg, Germany). Briefly, cells were suspended with 1× binding buffer at a concentration of 2×10^5 cells per 100 µL. Five µL of FITC annexin V and 5 µL propidium iodide (PI) were added to each solution and incubated for 20 minutes at room temperature (25°C) in the dark. Then, 200 µL of 1× binding buffer were added just before analysis by flow cytometry. A total of 10 000 cells by point were analyzed by fluorescence-assisted cell sorting flow cytometry at an excitation wavelength of 488 nm and emission wavelengths of 530 nm for FITC fluorescence and 610 nm for PI fluorescence. The percentage of viable (PI^-, $annexin^-$), apoptotic (PI^-, $annexin^+$) and necrotic cells (PI^+, $annexin^+$) were evaluated with CellQuestPro software (BD, Heidelberg, Germany). Since double labeling was performed, compensation was set using macrophages stained either with PI or with FITC-conjugated annexin V.

2.3.6 | Caspase-3 enzyme assay

Nr8383 cells were cultured (5×10^5/Petri dish) and exposed to CNTs (5, 10, 20 cm^2/cm^2 for MWCNT/NM403 and 4.5, 9, 19, 38 cm^2/cm^2 for SWCNT/NRCWE-055) for 24 hours. Activity of caspase-3 (CASP3) enzyme was determined using the EnzChek CASP3 fluorometric assay kit (molecular probes) with some modifications. In brief, cells were pelleted by centrifugation at 500 *g* for 5 minutes, washed twice with phosphate-buffered saline and incubated in 50 µL lysis buffer on ice for 30 minutes. The lysate was centrifuged at 5000 *g* for 5 minutes, and then 50 µL of supernatant was added to 50 µL of the reaction mixture and incubated for 30 minutes at room temperature. Fluorescence of the reaction mixture was measured at excitation/emission wavelengths of 430/535 nm using the FP-8300 Irm spectrofluorometer (Jasco).

2.3.7 | RNA extraction

After NR8383 cells treatment for 4 hours with the IC_{50} and $IC_{50/4}$ of each CNT, cells were lysed by adding 1 mL of Trizol Extraction Reagent (OMEGA Bio-Tek, Guang zhou, China), followed by the addition of 200 µL of chloroform (Carlo Erba reagents, Normandie, France). Samples were centrifuged at 800 *g* for 15 minutes and 500 µL of isopropanol (Carlo Erba reagents) was added to 350 µL of supernatant. The precipitates were subjected to two washing steps using ethanol 80% and incubated for 10 minutes at 60°C to remove ethanol, followed by dissolution in 35 µL RNase-free water.

RNA purity was assessed using a BioSpec-nano spectrophotometer (Shimadzu, Kyoto, Japan). In addition, the integrity of RNA was checked by RNA 6000 Nano Reagents Kit using Bioanalyzer™ 2100 (Agilent Technologies, Waldbron, Germany).

2.3.8 | Reverse transcription and quantitative real-time reverse transcription-polymerase chain reaction

For complementary DNA (cDNA) conversion, the iScript™ cDNA Synthesis Kit (Bio-Rad, Marnes-la-Coquette, France) was used according to the manufacturer's instructions. cDNA was stored at −20°C for later use. A mixture consisting of diluted cDNA, iQ™ SYBR Green® Supermix (Bio-Rad, France) and primer (Eurogentec, Marnes-la-Coquette Angers, France) for each gene was amplified by CFX Connect™ Real-Time system (Bio-Rad Laboratories, Singapore). For all the samples, an initial heat-denaturing step at 95°C for 5 minutes was followed by 40 cycles of 60°C for 1 minute and 95°C for 1 second. Gene expression levels were normalized by comparison to the ribosomal protein L13 (RPL13) housekeeping gene. Fold changes of gene expression were calculated by $2^{-\Delta\Delta CT}$ method.

2.4 | Statistical analysis

For viability tests the number of biological replicates (*N*) was four, the number of technical replicates (*n*) was six. Statistical differences were determined by an ANOVA one-way analysis of variance followed by Dunnett's test, using RLPlot software. Regarding quantitative reverse transcription-polymerase chain reaction ($N = 3$; $n = 2$), fold changes was calculated by the ratio of exposed/unexposed cells, and results were expressed as means ± SE. Statistical differences between control and exposed cells were determined by ANOVA followed by the Tukey-Kramer method.

3 | RESULTS

3.1 | Carbon nanotube physicochemical properties

The specific surface given by the provider was 135 m^2/g for MWCNT/NM403 and 436 m^2/g for SWCNT/NRCWE-055, as assessed by Brunauer-Emmett-Teller. The mean hydrodynamic diameter, determined by DLS from three independent preparations, was 217.2 ± 70.3 nm for MWCNT/NM403 and 601.7 ± 90.4 nm for SWCNT/NRCWE-055 with a polydispersity index of 0.383 ± 0.013 and 0.849 ± 0.025, respectively. The length calculated by transmission electron microscopy was 300 ± 90 nm for MWCNT/NM403 and 2 ± 1 µm for SWCNT/NRCWE-055 (Figure 1). Both CNTs displayed a zeta potential of −13.005 ± 0.025 mV.

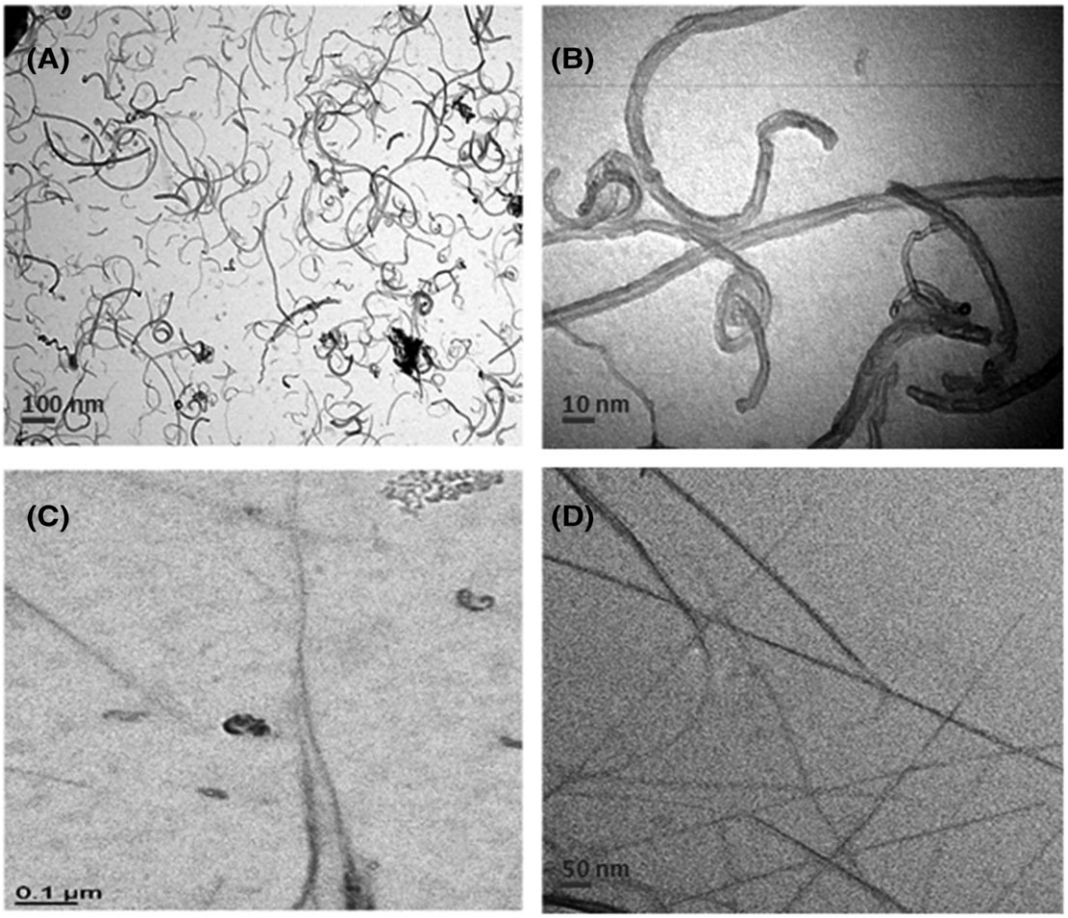

FIGURE 1 Transmission electron microscopy. A, B, Multiwall carbon nanotubes/NM403. C, D, Single wall carbon nanotubes/NRCWE-055

3.2 | Exposure to carbon nanotubes induced dose-dependent cytotoxicity in NR8383 cells

In NR8383 cells, according to the water-soluble tetrazolium salt assay test, 50% and 30% of cell death were observed respectively for the lowest doses, 2.5 cm^2/cm^2 of MWCNT/NM403 and 9 cm^2/cm^2 of SWCNT/NRCWE-055, after 24 hours of exposure. They decreased afterwards in a dose-dependent manner with only a slight difference between the results for both exposure times (4 and 24 hours). The IC_{50} was determined as 3.2 cm^2/cm^2 for MWCNT/NM403 and 44 cm^2/cm^2 for SWCNT/NRCWE-055.

We obtained similar results with the Alamar Blue test with small differences due to the sensibility of each test. The corresponding IC_{50} were 4.1 cm^2/cm^2 for MWCNT/NM403 and 41.2 cm^2/cm^2 for SWCNT/NRCWE-055 (Figure 2).

As far as the LDH test is concerned, there is a slightly significant increase (up to 30% compared to the negative control) after 24 hours of exposure to MWCNT/NM403 at high doses (10-80 cm^2/cm^2).

3.3 | Single wall carbon nanotube-induced apoptosis

Flow cytometry analysis, assayed by the FITC annexin V antibody is shown in Figure 3. Annexin V-$FITC^+$ and PI^- stain, in the lower-right quadrant, indicates the presence of apoptotic cells. Apoptosis increased from the lowest concentration of SWCNT/NRCWE-055 (9 cm^2/cm^2) to the highest concentration (75 cm^2/cm^2). For MWCNT/NM403, no such staining could be observed.

3.4 | No caspase-3 activation

Activation of the CASP3 pathway is a hallmark of apoptosis. However, in our study, CASP3 activation was not observed for any doses of MWCNT/NM403 and SWCNT/NRCWE-055 (data not shown).

3.5 | Gene expression analysis

A difference in gene expressions was observed with MWCNT/NM403 and SWCNT/NRCWE-055 (Table 1). For MWCNT/NM403, the *Tnf-α* and *Il-1β* genes related to inflammation were overexpressed after cell treatment while they were underexpressed in case of SWCNT. On the contrary, genes related to apoptosis (*Casp8*) or mitochondrial damage (*Opa*) were overexpressed after treatment with SWCNT/NRCWE-055 but not with MWCNT/NM403. Other genes, *Nfkb* and *Il-6* related to inflammation, *Ncf1* related to oxidative burst and *Bcl-2* and *Pdcd4* related to apoptosis, were similarly expressed, at low and high MWCNT/NM403 doses.

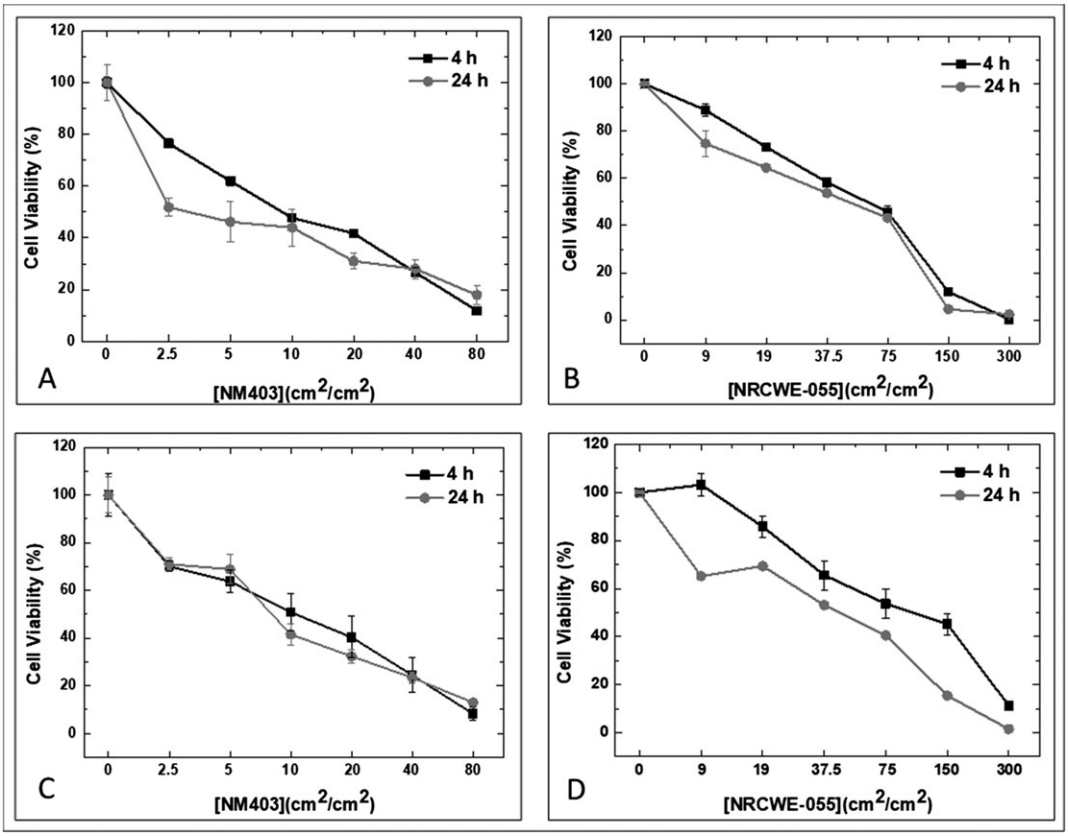

FIGURE 2 Cytotoxicity of carbon nanotubes on NR8383 cells. Toxicity was evaluated with two tests. A, C, Water-soluble tetrazolium salt assay test. B, D, Alamar Blue test. NR8383 cells were exposed to multiwall carbon nanotubes/NM403 (range 0-80 cm^2/cm^2) and to single wall carbon nanotubes/NRCWE-055 (range 0-300 cm^2/cm^2). Data represent the means ± SD of three independent experiments. $^*P < 0.05$, $^{**}P < 0.01$, $^{***}P < 0.001$ vs. non-treated cells. ANOVA was followed by Dunnett's multiple comparison test

4 | DISCUSSION

As we discussed at the beginning, in vivo studies have shown that CNTs induce immunologic and inflammatory responses. What seems promising, is to study the capacity of the in vitro model to predict the induction of these events. Hereby, we analyzed the expression of genes that play a major role in inflammation, oxidative burst, mitochondrial stress and cell death, following the exposure to two types of CNTs of different sizes: SWCNT/NRCWE-055 (thin and long) and MWCNT/NM403 (thick and short) on NR8383 cells. Macrophages (i.e., NR8383) are primary defenders against nanoparticles and principal actors for regulating the inflammatory response.

Indeed, a 30% decrease of cell viability in NR8383 was observed 24 hours after treatment with 150 cm^2/cm^2 of SWCNT/NRCWE-055. Fujita et al., reported similar data after 24 hours treating NR8383 cells with SWCNTs at the same dose (Fujita et al., 2015). Consequently, our results are in concordance with those of Fujita et al. However, for MWCNT/NM403, this was not the case. The literature reveals that MWCNTs do not produce a decrease in cell viability, which does not suit our results (Pulskamp et al., 2007). This variation may be due to differences in diameter of MWCNTs used in that study (30-50 nm), compared to MWCNT/NM403 we used (12 nm) in our study.

Overall, viability tests showed that MWCNT/NM403 are more cytotoxic than SWCNT/NRCWE-055. This confirms the hypothesis that thick nanomaterials are more toxic (Mrakovcic, Meindl, Leitinger, Roblegg, & Fröhlich, 2015).

CNTs are frequently reported to induce oxidative stress in lung cells (He, Young, Fernback, & Ma, 2012; Wang et al., 2016). Our results confirm that both SWCNTs and MWCNTs stimulate reactive oxygen species production at IC_{50} by superoxide bursts due to *Ncf* overexpression (Table 1).

However, at lower doses ($IC_{50/4}$), the *Ncf* gene was significantly overexpressed only after treatment with SWCNT/NRCWE-055. The overexpression of the *Ncf* gene at this concentration was accompanied by an overexpression of the *Opa* gene suggesting that SWCNT/NRCWE-055 induces mitochondrial damage. Park et al. (2014) demonstrated that SWCNTs produced reactive oxygen species in RAW264.7 macrophages and caused the lower production of ATP by damaging the mitochondrial function (Park et al., 2014). We therefore confirmed that SWCNT/NRCWE-055 induces oxidative stress and impairs mitochondria (He et al., 2012).

With MWCNT/NM403, no differential expression of *Opa* gene was observed, which is consistent with the Ghanbari et al. study. The latter also showed that MWCNTs produce less mitochondrial damage to cells than SWCNTs (Ghanbari et al., 2017), which coincides with our results (Supporting information).

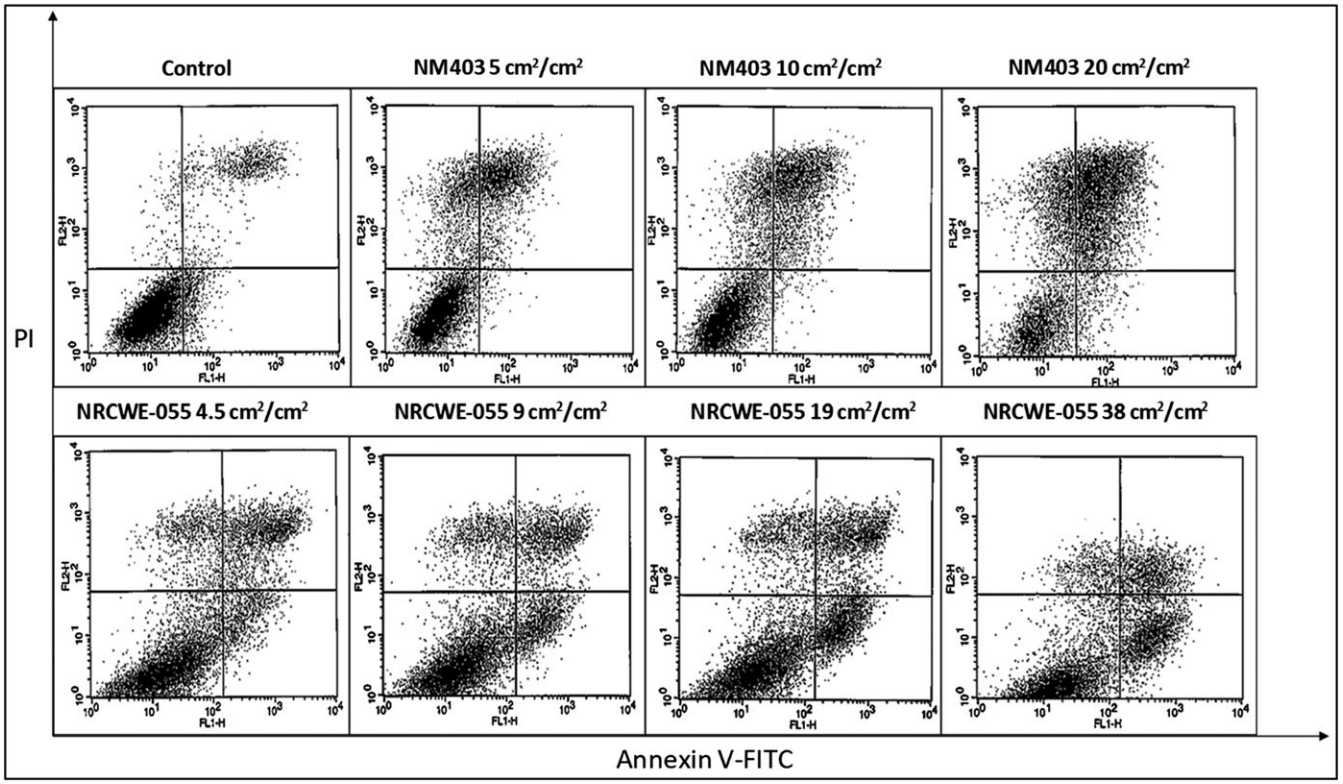

FIGURE 3 Flow cytometry results of the annexin V-FITC and PI assay. Cells stained with annexin V^-FITC^+ and PI^+ show up in the upper right quadrant. Cells stained with annexin V^-FITC^+ and PI^- show up in the lower right quadrant, whereas cells stained with annexin V^-FITC^- and PI^- show up in the lower left quadrant. A, Control group with no treatment. B, C, NR8383 cells exposed to multiwall carbon nanotubes/NM403 or single wall carbon nanotubes/NRCWE-055, respectively, for 24 h. FITC, fluorescein isothiocyanate; PI, propidium iodide

TABLE 1 Variation of gene expression after 4 h exposure of NR8383 cells to MWCNT/NM403 and SWCNT/NRCWE-055 ($IC_{50/4}$ and IC_{50}). Results were presented as fold change as compared to the control ± SE using ANOVA followed by Tukey-Kramer method

	Fold change							
	MWCNT/NM-403				SWCNT/NRCWE-055			
Genes	$IC_{50/4}$	*P* value	IC_{50}	*P* value	$IC_{50/4}$	*P* value	IC_{50}	*P* value
Ncf1	1.53 ± 0.2	NS	2.94 ± 0.1	<0.05	1.93 ± 0.3	<0.05	1.7 ± 0.1	<0.05
Opa	0.81 ± 0.1	<0.05	1.13 ± 0.1	NS	2.78 ± 0.3	<0.05	2.52 ± 0.2	NS
Nfkb	1.77 ± 0.3	NS	2.13 ± 0.3	NS	3.02 ± 0.3	NS	2.18 ± 0.2	NS
Tnfα	3 ± 0.2	<0.01	1.81 ± 0.2	<0.05	0.34 ± 0.1	<0.001	0.6 ± 0.1	<0.01
Il6	0.2 ± 0.04	<0.001	0.43 ± 0.1	<0.01	0.13 ± 0.1	<0.001	0.05 ± 0.1	<0.001
Il-1β	1.81 ± 0.1	<0.01	4.51 ± 0.3	<0.05	0.48 ± 0.1	<0.05	0.87 ± 0.1	NS
Pdcd4	0.62 ± 0.1	<0.05	0.64 ± 0.1	<0.05	0.65 ± 0.1	<0.05	0.71 ± 0.1	<0.05
Bcl2	0.31 ± 0.1	<0.05	0.7 ± 0.2	NS	0.36 ± 0.1	<0.01	0.26 ± 0.1	0.001
Casp8	0.54 ± 0.1	<0.05	0.74 ± 0.1	NS	2.11 ± 0.2	<0.05	1.16 ± 0.1	NS

MWCNT, multiwall carbon nanotube; NS, not significant; SWCNT, single wall carbon nanotube. Grey box, upregulated gene; white box, downregulated.

Previous studies have demonstrated that SWCNTs induce inflammation on NR8383 cells (Fujita et al., 2015), THP-1 and BEAS-2B cell lines (Wang et al., 2016). However, we did not find similar results with SWCNT/NRCWE-055.

On the other hand, MWCNT/NM403 induced an overexpression of *Tnf-α* and *Il-1β*. Therefore, MWCNTs induce inflammation as already assessed by the cDNA microarray (Table 1) (Hirano, Kanno, & Furuyama, 2008).

We can suggest the following hypothesis: MWCNTs lead to ROS production by inducing inflammation (Girardello, Baranzini, Tettamanti, de Eguileor, & Grimaldi, 2017) while SWCNTs enhance oxidative stress through mitochondrial damage as discussed earlier. (He et al., 2012).

In MWCNT/NM403-exposed cells, the flow cytometry experiment did not bring out any apoptosis characteristics, either at the protein level (CASP3), or at the mRNA level (*Casp8*). Both apoptosis-related

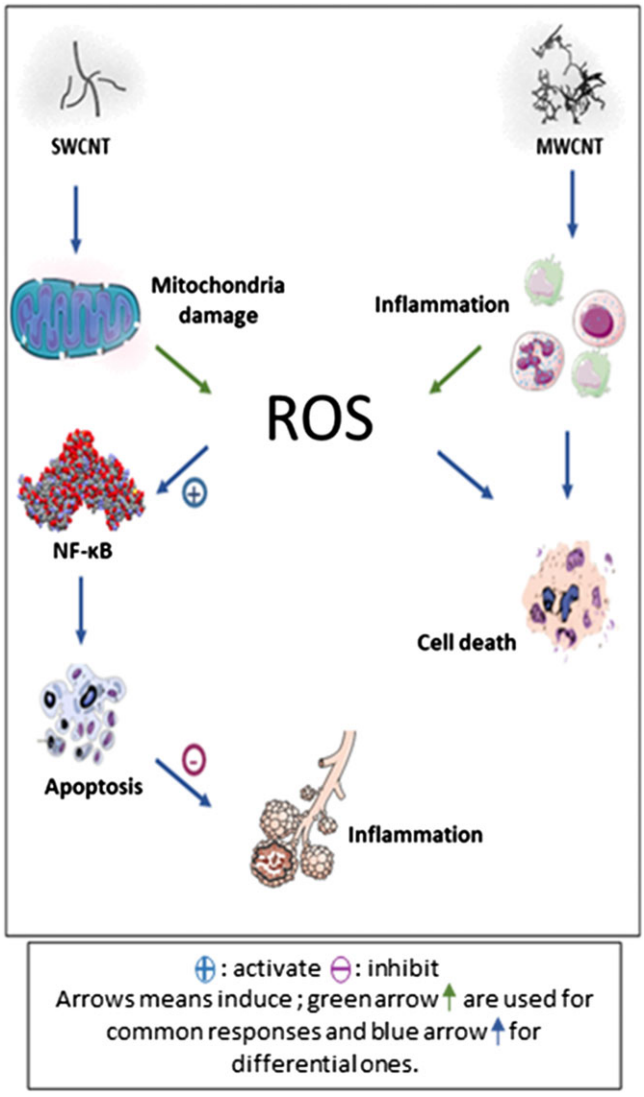

FIGURE 4 Schematic representation of two different pathways induced by SWCNT and MWCNT. MWCNT, multiwall carbon nanotube; NF-κB, nuclear factor kappaB; ROS, reactive oxygen species; SWCNT, single wall carbon nanotube [Colour figure can be viewed at wileyonlinelibrary.com]

genes (*Casp8* and *Pdcd4*) were slightly underexpressed. Otherwise, LDH release reveals NR8383 cell necrosis after 24 hours of exposure to MWCNTs (Chan, Moriwaki, & De Rosa, 2013). A few in vitro studies on cytotoxic effects of MWCNTs have been conducted. Indeed, Pulskamp et al. (2007) reported the absence of apoptosis after exposure to MWCNTs with similar characteristics to the ones we used in our study (Pulskamp et al., 2007). Likewise, Hirano et al. (2008) demonstrated the absence of apoptosis in J774.1 murine macrophage after treatment with MWCNTs. In another study, CASP3/7 were evaluated, and no activation in RAW 264.7 macrophages was reported after treatment with MWCNTs (Sohaebuddin, Thevenot, Baker, Eaton, & Tang, 2010). The occurrence of apoptosis in NR8383 cells exposed to SWCNT/NRCWE-055, shown by annexin V/IP staining, is supported by the overexpression of *Casp8*, as well as the expression of *Bcl-2*, both favoring apoptosis. The same response has been described with fibroblasts exposed to SWCNTs, which died by apoptosis (Cicchetti, Divizia, Valentini, & Argentin, 2011). In NR8383 cells, apoptosis caused by SWCNT/NRCWE-055 is CASP3 independent, as it did not trigger any significant synthesis of CASP3 protein.

However, apoptosis activation may be related to the presence of oxidative stress mediated by *Nfkb* expression in SWCNT/NRCWE-055-exposed cells. Indeed, this gene plays a crucial role in apoptosis activation, as proposed by Ravichandran and coworkers (Ravichandran et al., 2010). Consequently, SWCNT/NRCWE-055 induced the apoptosis via *Nfkb* signaling.

Thus, the fact that SWCNT/NRCWE-055 induced the apoptosis explained the absence of any inflammatory response after exposure to these SWCNTs. It is known that apoptotic cells stimulate an anti-inflammatory response that could explain the underexpression of genes coding for proinflammatory cytokines such as *Il-6*, *Il-1β* and *Bcl-2* as suggested by Szondy et al. (Szondy, Sarang, Kiss, Garabuczi, & Köröskényi, 2017). This phenomenon was previously seen in RAW 264.7 macrophages, which, exposed to 0.1 mg/mL SWCNT for 6 hours, produced fewer proinflammatory cytokines: interleukins 1β and 10, tumor necrosis factor-alpha and transforming growth factor-β1 (Shvedova et al., 2005). Therefore, SWCNT/NRCWE-055 induced apoptosis by activating *Nfkb*, which regulates NR8383 inflammatory response.

5 | CONCLUSION

While both MWCNT/NM403 and SWCNT/NRCWE-055 are cytotoxic, the former induces 13 times less cytotoxic effect than the latter (IC_{50} = 3.2 cm^2/cm^2 < IC_{50} = 44 cm^2/cm^2). Both induced oxidative bursts but in a different way. For MWCNT, it is related to an inflammatory response, while it seems to be related to a mitochondrial dysfunction in the case of SWCNT (Figure 4). With SWCNT/NRCWE-055, oxidative stress leads to apoptosis through *Nfkb* induction. Apoptotic cells then stimulate an anti-inflammatory response. Thus, despite a common chemical composition, notwithstanding the possible contamination (e.g., metal), the difference between both CNTs is related, on the one hand, to their specific surface property (increased in MWCNTs vs. SWCNTs), and on the other hand, to their different length property (higher for SWCNTs). We suggest the presence of a relationship between cell death pathways, CNT physicochemical characteristics, and induction of acute inflammation in vivo. Further studies will be done in this sector.

ACKNOWLEDGMENTS

The authors would like to acknowledge Justine Paoli for kind assistance with electron microscopy imaging and Smartnanotox partners for nanomaterial characterization. This work has received funding from the European Union's Horizon 2020 research (SmartNanotox project) and innovation program.

CONFLICTS OF INTEREST

The authors have no conflicts of interest to report.

ORCID

Sara Nahle https://orcid.org/0000-0001-9853-709X

REFERENCES

Allegri, M., Perivoliotis, D. K., Bianchi, M. G., Chiu, M., Pagliaro, A., Koklioti, M. A., … Charitidis, C. A. (2016). Toxicity determinants of multi-walled carbon nanotubes: The relationship between functionalization and agglomeration. *Toxicology Reports*, *3*, 230–243. https://doi.org/10.1016/j.toxrep.2016.01.011

Assali, M., Zaid, A. N., Abdallah, F., Almasri, M., & Khayyat, R. (2017). Single-walled carbon nanotubes-ciprofloxacin nanoantibiotic: strategy to improve ciprofloxacin antibacterial activity. *International Journal of Nanomedicine*, *12*, 6647–6659. https://doi.org/10.2147/IJN.S140625

Boyles, M. S. P., Young, L., Brown, D. M., MacCalman, L., Cowie, H., Moisala, A., … Stone, V. (2015). Multi-walled carbon nanotube induced frustrated phagocytosis, cytotoxicity and pro-inflammatory conditions in macrophages are length dependent and greater than that of asbestos. *Toxicology In Vitro: An International Journal Published in Association with BIBRA*, *29*(7), 1513–1528. https://doi.org/10.1016/j.tiv.2015.06.012

Chan, F. K.-M., Moriwaki, K., & De Rosa, M. J. (2013). Detection of necrosis by release of lactate dehydrogenase activity. *Methods in Molecular Biology (Clifton, N.J.)*, *979*, 65–70. https://doi.org/10.1007/978-1-62703-290-2_7

Cicchetti, R., Divizia, M., Valentini, F., & Argentin, G. (2011). Effects of single-wall carbon nanotubes in human cells of the oral cavity: genocytotoxic risk. *Toxicology In Vitro: An International Journal Published in Association with BIBRA*, *25*(8), 1811–1819. https://doi.org/10.1016/j.tiv.2011.09.017

Dresselhaus, M. S., Dresselhaus, G., Charlier, J. C., & Hernández, E. (2004). Electronic, thermal and mechanical properties of carbon nanotubes. *Philosophical Transactions. Series A, Mathematical, Physical, and Engineering Sciences*, *362*(1823), 2065–2098. https://doi.org/10.1098/rsta.2004.1430

Duke, K. S., Taylor-Just, A. J., Ihrie, M. D., Shipkowski, K. A., Thompson, E. A., Dandley, E. C., … Bonner, J. C. (2017). STAT1-dependent and -independent pulmonary allergic and fibrogenic responses in mice after exposure to tangled versus rod-like multi-walled carbon nanotubes. *Particle and Fibre Toxicology*, *14*(1), 26. https://doi.org/10.1186/s12989-017-0207-3

Ema, M., Takehara, H., Naya, M., Kataura, H., Fujita, K., & Honda, K. (2017). Length effects of single-walled carbon nanotubes on pulmonary toxicity after intratracheal instillation in rats. *The Journal of Toxicological Sciences*, *42*(3), 367–378. https://doi.org/10.2131/jts.42.367

Fujita, K., Fukuda, M., Endoh, S., Maru, J., Kato, H., Nakamura, A., … Honda, K. (2015). Size effects of single-walled carbon nanotubes on in vivo and in vitro pulmonary toxicity. *Inhalation Toxicology*, *27*(4), 207–223. https://doi.org/10.3109/08958378.2015.1026620

Ge, C., Li, Y., Yin, J.-J., Liu, Y., Wang, L., Zhao, Y., & Chen, C. (2012). The contributions of metal impurities and tube structure to the toxicity of carbon nanotube materials. *NPG Asia Materials*, *4*(12), e32. https://doi.org/10.1038/am.2012.60

Ghanbari, F., Nasarzadeh, P., Seydi, E., Ghasemi, A., Taghi Joghataei, M., Ashtari, K., & Akbari, M. (2017). Mitochondrial oxidative stress and dysfunction induced by single- and multiwall carbon nanotubes: A comparative study. *Journal of Biomedical Materials Research. Part A*, *105*(7), 2047–2055. https://doi.org/10.1002/jbm.a.36063

Girardello, R., Baranzini, N., Tettamanti, G., de Eguileor, M., & Grimaldi, A. (2017). Cellular responses induced by multi-walled carbon nanotubes: in vivo and in vitro studies on the medicinal leech macrophages. *Scientific Reports*, *7*(1), 8871. https://doi.org/10.1038/s41598-017-09011-9

He, X., Young, S.-H., Fernback, J. E., & Ma, Q. (2012). Single-walled carbon nanotubes induce fibrogenic effect by disturbing mitochondrial oxidative stress and activating NF-κB signaling. *Journal of Clinical Toxicology*, (Suppl 5). https://doi.org/10.4172/2161-0495.S5-005

Hirano, S., Kanno, S., & Furuyama, A. (2008). Multi-walled carbon nanotubes injure the plasma membrane of macrophages. *Toxicology and Applied Pharmacology*, *232*(2), 244–251. https://doi.org/10.1016/j.taap.2008.06.016

Khan, A. S., Hussain, A. N., Sidra, L., Sarfraz, Z., Khalid, H., Khan, M., … Rehman, I. U. (2017). Fabrication and in vivo evaluation of hydroxyapatite/carbon nanotube electrospun fibers for biomedical/dental application. *Materials Science & Engineering. C, Materials for Biological Applications*, *80*, 387–396. https://doi.org/10.1016/j.msec.2017.05.109

Lefebvre, J., Ding, J., Li, Z., Finnie, P., Lopinski, G., & Malenfant, P. R. L. (2017). High-purity semiconducting single-walled carbon nanotubes: a key enabling material in emerging electronics. *Accounts of Chemical Research*, *50*(10), 2479–2486. https://doi.org/10.1021/acs.accounts.7b00234

Madian, M., Ummethala, R., Naga, A. O. A. E., Ismail, N., Rümmeli, M. H., Eychmüller, A., & Giebeler, L. (2017). Ternary CNTs@TiO_2/CoO nanotube composites: improved anode materials for high performance lithium ion batteries. *Materials (Basel, Switzerland)*, *10*(6). https://doi.org/10.3390/ma10060678

Messina, E., Leone, N., Foti, A., Di Marco, G., Riccucci, C., Di Carlo, G., … Gucciardi, P. G. (2016). Double-wall nanotubes and graphene nanoplatelets for hybrid conductive adhesives with enhanced thermal and electrical conductivity. *ACS Applied Materials & Interfaces*, *8*(35), 23244–23259. https://doi.org/10.1021/acsami.6b06145

Monea, B. F., Ionete, E. I., Spiridon, S. I., Leca, A., Stanciu, A., Petre, E., & Vaseashta, A. (2017). Single wall carbon nanotubes based cryogenic temperature sensor platforms. *Sensors (Basel, Switzerland)*, *17*(9). https://doi.org/10.3390/s17092071

Mrakovcic, M., Meindl, C., Leitinger, G., Roblegg, E., & Fröhlich, E. (2015). Carboxylated short single-walled carbon nanotubes but not plain and multi-walled short carbon nanotubes show in vitro genotoxicity. *Toxicological Sciences: An Official Journal of the Society of Toxicology*, *144*(1), 114–127. https://doi.org/10.1093/toxsci/kfu260

Park, E.-J., Zahari, N. E. M., Kang, M.-S., Lee, S. j., Lee, K., Lee, B.-S., … Kim, J.-H. (2014). Toxic response of HIPCO single-walled carbon nanotubes in mice and RAW264.7 macrophage cells. *Toxicology Letters*, *229*(1), 167–177. https://doi.org/10.1016/j.toxlet.2014.06.015

Pitkethly, M. J. (2004). Nanomaterials—the driving force. *Materials Today*, *7*(12, Supplement), 20–29. https://doi.org/10.1016/S1369-7021(04)00627-3

Poulsen, S. S., Jackson, P., Kling, K., Knudsen, K. B., Skaug, V., Kyjovska, Z. O., … Vogel, U. (2016). Multi-walled carbon nanotube physicochemical properties predict pulmonary inflammation and genotoxicity. *Nanotoxicology*, *10*(9), 1263–1275. https://doi.org/10.1080/17435390.2016.1202351

Pulskamp, K., Diabaté, S., & Krug, H. F. (2007). Carbon nanotubes show no sign of acute toxicity but induce intracellular reactive oxygen species in dependence on contaminants. *Toxicology Letters*, *168*(1), 58–74. https://doi.org/10.1016/j.toxlet.2006.11.001

Qin, Y., Li, S., Zhao, G., Fu, X., Xie, X., Huang, Y., … Lai, Z. (2017). Long-term intravenous administration of carboxylated single-walled carbon nanotubes induces persistent accumulation in the lungs and pulmonary fibrosis via the nuclear factor-kappa B pathway. *International Journal of Nanomedicine*, *12*, 263–277. https://doi.org/10.2147/IJN.S123839

Ravichandran, P., Baluchamy, S., Sadanandan, B., Gopikrishnan, R., Biradar, S., Ramesh, V., … Ramesh, G. T. (2010). Multiwalled carbon nanotubes activate NF-κB and AP-1 signaling pathways to induce apoptosis in rat lung epithelial cells. *Apoptosis: An International Journal on Programmed Cell Death*, *15*(12), 1507–1516. https://doi.org/10.1007/s10495-010-0532-6

Samadishadlou, M., Farshbaf, M., Annabi, N., Kavetskyy, T., Khalilov, R., Saghfi, S., … Mousavi, S. (2017). Magnetic carbon nanotubes:

preparation, physical properties, and applications in biomedicine. *Artificial Cells, Nanomedicine, and Biotechnology*, 1–17. https://doi.org/10.1080/21691401.2017.1389746

Shvedova, A. A., Kisin, E. R., Mercer, R., Murray, A. R., Johnson, V. J., Potapovich, A. I., … Baron, P. (2005). Unusual inflammatory and fibrogenic pulmonary responses to single-walled carbon nanotubes in mice. *American Journal of Physiology. Lung Cellular and Molecular Physiology*, *289*(5), L698–L708. https://doi.org/10.1152/ajplung.00084.2005

Sohaebuddin, S. K., Thevenot, P. T., Baker, D., Eaton, J. W., & Tang, L. (2010). Nanomaterial cytotoxicity is composition, size, and cell type dependent. *Particle and Fibre Toxicology*, *7*, 22. https://doi.org/10.1186/1743-8977-7-22

Szondy, Z., Sarang, Z., Kiss, B., Garabuczi, É., & Köröskényi, K. (2017). Anti-inflammatory mechanisms triggered by apoptotic cells during their clearance. *Frontiers in Immunology*, *8*. https://doi.org/10.3389/fimmu.2017.00909

Vales, G., Rubio, L., & Marcos, R. (2016). Genotoxic and cell-transformation effects of multi-walled carbon nanotubes (MWCNT) following in vitro sub-chronic exposures. *Journal of Hazardous Materials*, *306*, 193–202. https://doi.org/10.1016/j.jhazmat.2015.12.021

Wang, X., Mansukhani, N. D., Guiney, L. M., Lee, J.-H., Li, R., Sun, B., … Nel, A. E. (2016). Toxicological profiling of highly-purified metallic and semiconducting single-walled carbon nanotubes in the rodent lung and *E. coli*. *ACS Nano*, *10*(6), 6008–6019. https://doi.org/10.1021/acsnano.6b01560

SUPPORTING INFORMATION

Additional supporting information may be found online in the Supporting Information section at the end of the article.

How to cite this article: Nahle S, Safar R, Grandemange S, et al. Single wall and multiwall carbon nanotubes induce different toxicological responses in rat alveolar macrophages. *J Appl Toxicol*. 2019;1–9. https://doi.org/10.1002/jat.3765